激光与光电子学进展

Super-Resolution Fluorescence Microscopy for Cilia Investigation and Ciliopathy Diagnosis (Invited)

Liu Zhen, Wu Yang

Division of Life Science, The Hong Kong University of Science and Technology, Hong Kong, China

Abstract　The last two decades have witnessed the invention and development of super-resolution microscopy (SRM) that breaks the diffraction limit of light and pushes the fluorescence microscopy resolution to several nanometers. While SRM is widely used in biological studies, such as resolving subdiffraction structures, molecular mapping, tracking single molecules, probing protein-protein interactions, and observing organelle dynamics, its direct application in translational medicine, such as disease diagnosis, is still preliminary. Despite their small size, cilia play a crucial role as organelles in cell signaling and motility, with defects in cilia leading to ciliopathy. Similar to other miniature organelles and macromolecular complexes, cilia are ideal for super-resolution imaging. In this review, we will 1) introduce cilia and ciliopathy, 2) show how SRM extends our knowledge of cilia, and 3) focus on how SRM improves the diagnosis of motile ciliopathies.

1　Introduction

Fluorescence microscopy has been extensively used in biological research due to its molecular specificity, live-cell compatibility, and multicolor observation[1-2]. However, due to diffraction of light, the resolution of fluorescence microscopy is limited to ~250 nm, impeding researchers from observing the mechanism below the diffraction limit. Super-resolution microscopy (SRM) has emerged as a collection of techniques that break the diffraction limit and push the optical resolution to several nanometers, enabling the visualization of subdiffraction cellular structures.

Based on different principles, as shown in Fig. 1, there are generally five groups of super-resolution imaging techniques. 1) The first relies on the precise localization of well-separated single molecules with nanometer accuracy. By stochastically activating a subset of spatially well-separated single fluorophores and sequentially imaging these single-molecule events, a final super-resolution image can be constructed by rendering all molecule coordinates on an image. This group is called single-molecule localization microscopy (SMLM) and includes stochastic optical reconstruction

microscopy (STORM)[3-4], (fluorescence) photoactivated localization microscopy ((f)PALM)[5-6], and DNA point accumulation for imaging in nanoscale topography (DNA-PAINT)[7-8]. Typical commercial SMLM setups can achieve a resolution of ~20 nm. 2) The second approach involves engineering the illumination light pattern. Structured illumination microscopy (SIM)[9-10] adapts patterned light, such as sine waves, to interfere with the sample signal to introduce the Moiré effect, which brings invisible high-frequency information to the observable low-frequency domain[11]. SIM routinely reaches a resolution of ~120 nm. 3) Stimulated emission depletion (STED)[12]/reversible saturable optical fluorescence transitions (RESOLFT)[13-14] introduces a donut-shaped depletion laser to trim the diffraction spot for scanning, creating a substantially smaller excitation spot to scan the sample. The resolution of STED/RESOLFT is ~50 nm.

Two other techniques—super-resolution optical fluctuation imaging (SOFI) and expansion microscopy—also achieve super-resolution imaging. 4) SOFI uses the intrinsic fluctuation properties of fluorophores and is a computational technique that relies on the post-data analysis of the fluorescence signal correlation to achieve
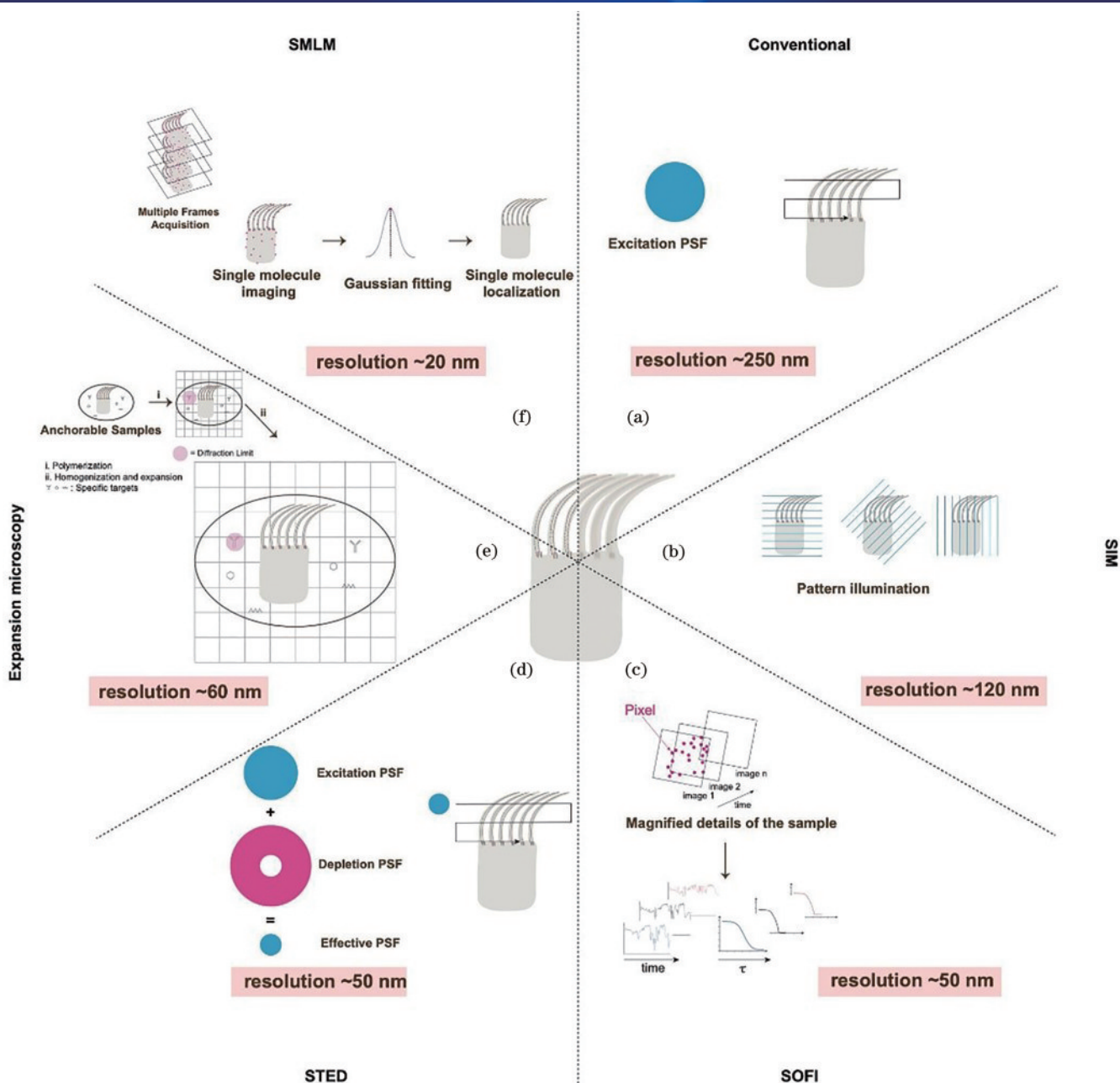
Fig. 1 Summary of different super-resolution imaging techniques. (a) Conventional imaging; (b) SIM; (c) SOFI; (d) STED; (e) expansion microscopy; (f) SMLM

enhanced resolution[15]. The simplest second-order SOFI offers a $\sqrt{2}$ fold increase in resolution and is particularly suitable for live cell imaging. 5）Expansion microscopy[16-17]，different from all other approaches, uses swelling gels to embed samples and physically expand cells or tissues in all directions. Expansion microscopy achieves a resolution of ~60 nm using a conventional microscope，and the latest version can expand samples ~20 fold，realizing a resolution of ＜10 nm[18].

Recent developments in super-resolution microscopy involve the combination of different techniques to achieve sub-10-nm resolution or molecular resolution. MINFLUX[19] is such an example that uses a donut-shaped excitation laser rather than a depletion laser to scan a fluorescent molecule to determine its center position，which requires significantly fewer photons yet provides nanometer accuracy. Similar to SMLM，by introducing photoswitchable fluorescent molecules, MINFLUX can sequentially localize molecules and realize super-resolution imaging with several nanometer resolutions.

The range of tools available for super-resolution imaging is expanding，with each offering distinct characteristics to meet various needs in biological research，such as higher spatial and/or temporal resolution，multiplexed labeling，reduced phototoxicity,

and extended sample depth. In summary, these techniques have dramatically altered fluorescence microscopy and pushed it to the nanoscopy era, revolutionizing the field of biology.

2 Cilia and ciliopathy

Cilia are hair-like slender cellular organelles that arise from membrane-docked centrioles and protrude from the surface of the cell. Cilia can be motile or sensory depending on whether they beat or not.

Generally, sensory cilia are solitary and critical for signal perception and transduction. One example is the photoreceptor outer segment, which is a specialized cilium for photon reception. Sensory cilia appear in nearly all human cells and function in signaling pathways, such as Hedgehog (Hh), GPCR, RTK, and WNT signaling[20]. Recent studies reported that sensory cilia have diverse functions, such as controlling appetite[21], regulatig circadian clock[22], and forming axon-cilium synapses[23].

Motile cilia also possess sensory functions but are designed specifically for fluid propelling or cell motility. Motile cilia are present along the airway epithelia, brain ventricular wall, and female fallopian tube to remove mucus, circulate cerebrospinal fluids, and deliver zygotes[24-26]. Mucociliary clearance is the primary innate immunity mechanism in the airways[27]: airway cilia beat continuously in a coordinated metachronous pattern to eliminate mucus-trapped pathgogens[28]. In the central nervous system, the synchronized beating of ependymal cilia plays an indispensable role in the directional flow of cerebrospinal fluid[29]. Sperm cells move along the female reproductive system and are locomoted by a specialized cilium (flagellum), and motile cilia cover the epithelia of the fallopian tube[26].

Cilia defects lead to ciliopathies, a collection of rare diseases that affect nearly all human organs, including symptoms such as blindness, obesity, kidney abnormalities, and/or mental retardation[30]. While certain ciliopathies mainly affect one organ, others affect nearly all organs, examples being patients with Bardet-Biedl syndrome who suffer from vision loss, obesity, polydactyly, intellectual problems, and infertility. Despite their rarity, because of the variety of ciliopathies, the cumulative prevalence reaches ~1 in 2000 populations[31].

Dysfunctions of motile cilia lead to motile ciliopathies[26], as shown in Fig. 2(a). Motile ciliopathy manifestations can range from otosino pulmonary diseases, laterality defects, and male/female infertility to multisystem disorders, such as primary ciliary dyskinesia (PCD), which despite being rare is the most common motile ciliopathy[32-34]. Genetic mutations that impair the cilia beat are the main causes of motile ciliopathies. PCD is genetically heterogeneous: ~56 causative genes (by October 2023) have been reported and more are being discovered. PCD is estimated to affect ~1 in 7500 people[35]. Based on the incidence rate and the global population (2023), there are ~4 million ciliopathy patients globally and ~1 million patients
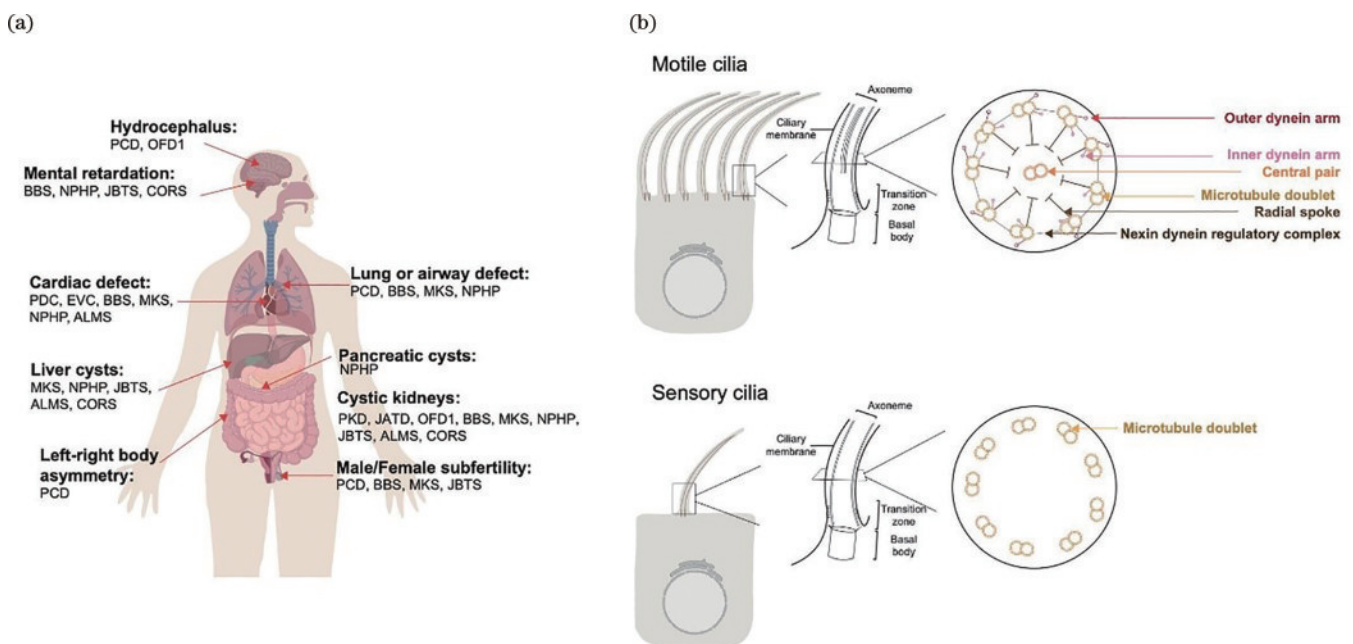

Fig. 2 Cilia and ciliopathy. (a) Cilia and affected organs; (b) structure of sensory and motile cilia

suffer from PCD.

3 Size and architecture of cilia

For long, cilia have been regarded as futile, partly because of their small size. Despite their small size, cilia possess a delicate architecture. The centriole first docks on the plasma membrane through its distal appendage and forms the basal body of cilia, which are approximately 200-nm wide and 300–500-nm long. Cilia then build the transition zone, a diffusion barrier that gates the ciliary contents, and the membrane-encased nine-microtubule-based axoneme grows from the transition zone. Intraflagellar anterograde and retrograde transport shuttles ciliary components into and out of cilia, building cilia and maintaining their functions. The cilia diameter is approximately 80–200 nm, and their lengths vary from 2 to 10 μm. For motile cilia, most have two microtubule central singlets and molecular motors, such as outer dynein arm (ODA) and inner dynein arm (IDA) complexes, surrounding the microtubule doublet and power the cilia beat, as shown in Fig. 2(b). The nexin-dynein regulatory complex (NDRC) links nine microtubule doublets, and the radial spoke (RS) links nine microtubules to the two central singlet complexes[24]. The cilia tip is capped with a specialized crown structure, and the ciliary membrane is enriched with membrane proteins for signal transduction. Thus, the sophisticated architecture of cilia supports their diversified and critical functions.

4 Super-resolution microscopy boosts research

Sensory cilia have long been ignored until the discovery of their role in Hh signaling[36]. Although transmission electron microscopy (TEM) can distinguish different subciliary structures such as the axoneme and transition zone, it lacks molecular specificity and fails to reveal the spatial organization of the ciliary proteome, which is estimated to possess >200 proteins[37]. Motile cilia are a hot spot for cryo-electron microscopy/ tomography (cryo-EM[38]/ET)[39], which have revealed the molecular architecture of the axoneme by averaging the periodic pattern along the axoneme[40]. However, this method uses purified cilia components and sacrifices the heterogeneity among microtubule doublets. Notably, the transition zone and ciliary membrane components have a highly organized architecture. Although conventional fluorescence microscopy can locate proteins in cilia, it fails to reveal protein organization within cilia due to resolution limit. To our delight, super-resolution imaging provides a powerful tool for interrogating these questions *in situ*. To date, SMLM, SIM, and STED have been successfully used to investigate the subciliary architecture, such as the diffusion barrier, basal foot, ciliary membrane, and axoneme. More recently, expansion microscopy and the combination of different super-resolution imaging techniques have emerged to further boost cilia research and aid the diagnosis of ciliopathies, such as Joubert syndrome (JS) and PCD.

4.1 Diffusion barrier

To maintain the cilia's unique composition, a diffusion barrier gates the transport of ciliary components. The diffusion barrier sits at the base of cilia and comprises the transition zone, transition fiber, and the region in between. The transition zone is characterized by a Y link that connects the axoneme and ciliary membrane. Transition zone defects lead to ciliopathies, such as JS, Meckel-Gruber syndrome (MKS), and nephronophthisis (NPHP).

The transition zone contains at least 26 proteins[41-42], which can be grouped into three modules: MKS, NPHP, and CEP290. In 2015, Yang *et al.*[43] first investigated the organization of the transition zone components by STED, as shown in Fig. 3(a). Using image averaging and overlaying with electron microscopy micrographs, they found that CEP290 bridges the basal body and other transition zone components, such as the MKS and NPHP modules. The MKS module transmembrane proteins TMEM67, TCTN2, and MKS1 localize to the same axial level as the RPGRIP1L module, which is closer to the axoneme. Subsequently, Shi *et al.*[44] reexamined transition zone organization using STORM and found that the MKS and NPHP modules form rings of discrete puncta. By aligning the images and examining the angular position histogram, the authors further discovered that both NPHP and MKS complexes form nine-fold symmetric doublets, as shown in Fig. 3(b), which is consistent with the Y links observed by TEM, whereas STORM result reveals the distribution of specific proteins. The Y link connects the axoneme core and the membrane, forming a periodic structure called the ciliary necklace. The short transition zone length poses a challenge for super-resolution imaging. Notably, the transition zone within certain species or cell types is significantly longer. Lambacher *et al.*[45] first examined the transition zone of *Carnorhabditis elegans* sensory cilia
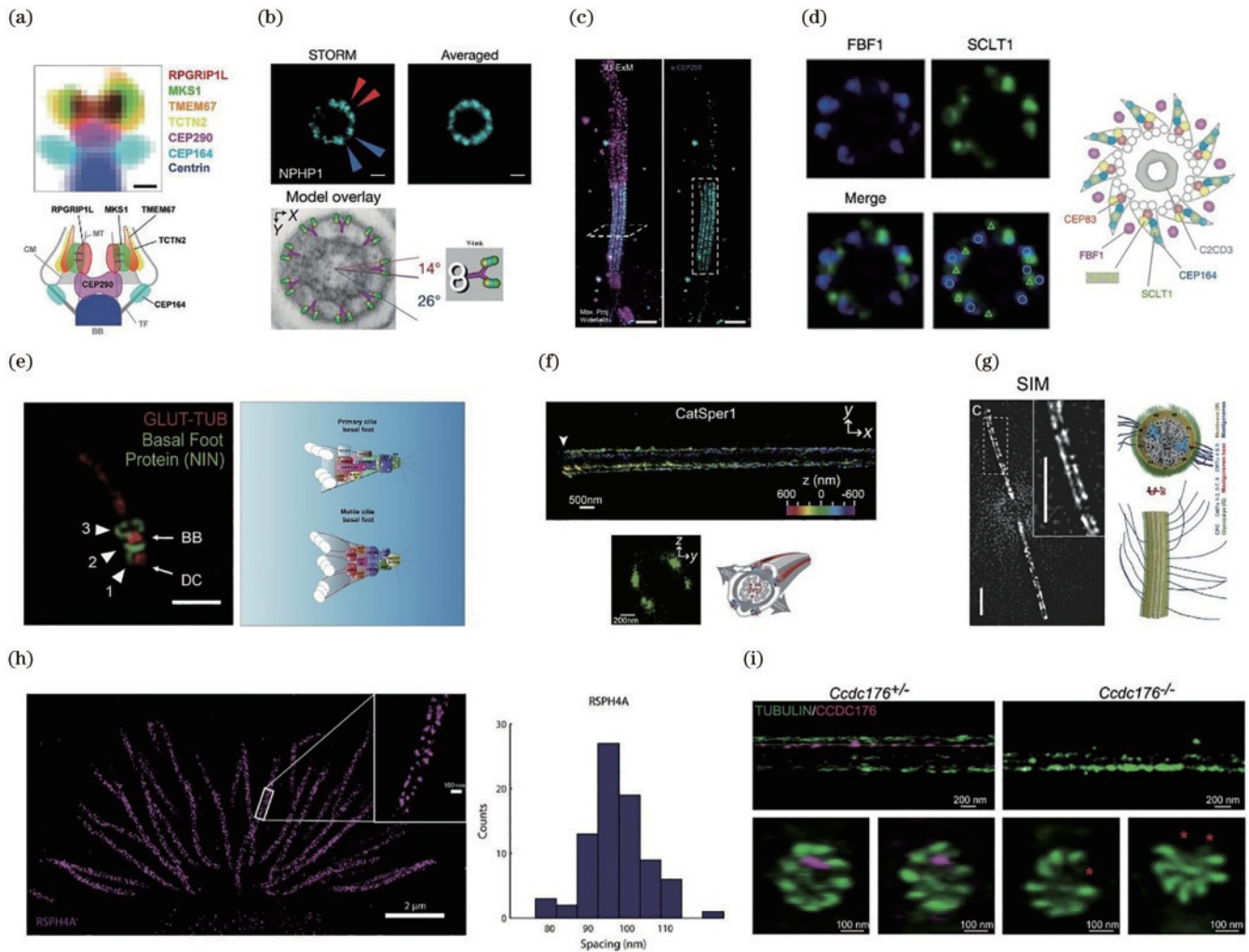
Fig. 3　Super-resolution imaging resolves ciliary architecture. (a)–(c) Transition zone architecture revealed by STED[43], STORM[44], and expansion microscopy[48]; (d) STORM reveals an unexpected matrix zone for the transition fiber[43]; (e) organization of basal foot proteins in both sensory and motile cilia revealed by three-dimensional (3D) SIM[50]; (f) STORM shows that CatSper1 forms four linear domains along the sperm flagella[55]; (g) SIM reveals that *Chlamydomonas* PKD2 forms two linear domains and associates with doublets 4 and 8[57]; (h) STORM reveals the 96-nm periodicity of the RS component RSPH4A[40]; (i) ROSE-Z shows that CCDC176 binds and stabilizes doublets 1 and 9[58]

and discovered the periodic pattern of TMEM231 and NPHP1 along the cilia axis by STED. The photoreceptor connecting cilia（CC）is an extremely long type of transition zone. Using (iterative) ultrastructure expansion microscopy, Lancaster *et al.* and Louvel *et al.* [46-48] revealed the necklace pattern of CEP290 along the mouse CC, as shown in Fig. 3(c).

　　Yang *et al.* also resolved the organization of the transition fiber, another diffusion barrier of cilia. Under TEM micrographs, the transition fiber appears as nine-fold blades emanating from the basal body. By examining 16 transition fiber components, they found that these proteins form a cone-shaped structure with proteins, such as FBF1, located in the space between the blades, a new structure not previously recognized by TEM, as shown in Fig. 3(d). They further named

the new structure the distal appendage matrix. This study further highlights that super-resolution microscopy can reveal structures ambiguous to TEM. Later, using correlative STORM and TEM, Bowler *et al.* [49] accurately determined the relative position of distal appendage proteins to both the centriole microtubule and transition fiber electron densities.

4.2　Basal foot

　　The basal foot is a macromolecular structure of the basal body that originates from the subdistal appendage of the centriole. Unlike the transition fiber, which exhibits a 9-fold symmetry, the number of basal feet per cilium varies among different cell types and depends on different factors[50-51]. The sensory cilia basal foot participates in TGFbeta-signaling, and its components keep cilia merged in the ciliary pocket[52-53]. The basal

feet of the motile cilia are important for coordinating the motile cilia beat. TEM reveals that the basal foot has a conical structure; however, how basal foot proteins are organized remains unclear. Nguyen et al.[50] reported the structure of the basal foot by examining its known components. Using 3D SIM, they found that the basal foot forms three modular regions: the basal foot anchoring domain, scaffolding domain, and MT anchoring domain [Fig. 3(e)]. They further used protein-domain-specific proximity labeling and super-resolution imaging to identify the new basal foot protein CEP112. By comparing the basal foot of sensory and motile cilia, Nguyen et al.[50-51] found cilia-specific organization of the basal foot. This comparative study led to the discovery of a novel hybrid type of cilia in multiciliated cells, whose basal feet are similar to primary cilia, whereas the axoneme has a typical 9+2 motile cilia configuration.

4.3　Ciliary membrane protein

　　Membrane proteins have peculiar organizations, such as protein islands and functional domains. Recent research explored if ciliary membrane proteins have similar distributions. Yoon et al.[54] first examined the nanoscale morphology of primary cilia by imaging the ciliary membrane protein Smoothened (SMO). Through surface reconstruction, they found significant heterogeneity, such as deformations not visible through conventional fluorescence microscopy. Interestingly, some specific ciliary membrane proteins distributions were discovered along the axis of the sperm flagellum. CatSper is a sperm-specific calcium channel whose activation is critical for fertilization. Using STORM, Chung et al.[55] revealed that CatSper forms four strip-like domains along the flagellum, as shown in Fig. 3(f). Functional research suggests that this organization is essential for organizing signaling proteins and confining tyrosine phosphorylation to the flagellar core. Similarly, Miller et al.[56] found that Hv1, a sperm proton channel, distributes as two lines asymmetrically along the sperm flagellum and functions in sperm rotation. Liu et al.[57] examined the distribution of PKD2, a cation channel associated with polycystic kidney disease, along with *Chlamydomonas* flagella. Surprisingly, they found that PKD2 is organized as two arrays that physically link to axonemal doublets 4 and 8, the orientation of which is perpendicular to the cilia beat plane, as shown in Fig. 3(g). Furthermore, they found that PKD2 is crucial for anchoring glycoproteins to the cilia surface. The surface of human airway motile cilia has glycoproteins. It would be interesting to explore whether this structure is conserved in human motile cilia. There have been no reports of peculiar motile cilia membrane protein distribution; however, because motile cilia beat asymmetrically along the beat plane, the asymmetrical distribution of certain ciliary membrane proteins is highly probable.

4.4　Ciliary axoneme

　　The distribution of axoneme accessory proteins, such as ODAs and IDAs forms periodic structures. For instance, ODAs form 32-nm repeats, whereas IDAs, NDRC, and RS proteins form 96-nm repeats[24]. This rhythmic distribution is highlighted by cryo-EM/ET but not by fluorescence microscopy due to resolution limit. Liu et al.[40] first observed the 96-nm periodic pattern of the RS component RSPH4A [Fig. 3(h)] and the NDRC component GAS8 using STORM. Another fascinating question is whether a doublet-specific protein distribution exists because motile cilia beat asymmetrically. Liu et al.[58] identified the protein CCDC176 specifically located in microtubule doublets 1 and 9 by ROSE-Z, a super-resolution imaging technique that combines STORM and SIM to achieve sub-10-nm resolution. Further knockout of CCDC176 in mouse sperm showed that CCDC176 is important for stabilizing doublets 1 and 9, as shown in Fig. 3(i).

5　Ciliopathy investigation and diagnosis using super-resolution microscopy

5.1　Joubert syndrome study using SIM

　　JS is a rare ciliopathy with symptoms of brain abnormalities characterized by the molar tooth sign under nuclear magnetic resonance imaging. JS is genetically heterogeneous, and a large portion of the disease-causative genes encode transition zone components. The molecular mechanism of JS is unclear. Using STORM, Shi et al. examined the fibroblast cilia transition zone from patients with JS bearing either *TCTN2* or *RPGRIP1L* mutations. Interestingly, they found that the MKS and NPHP complexes are absent from the patients' cells, suggesting that transition zone absence might be a common feature [Fig. 4(a)]. Cilia are important for developmental pathways, such as Hh signaling, and the transition zone plays a critical role in shuttling signaling proteins into and out of cilia. Shi et al. further investigated whether Hh signaling is disrupted in JS. In control fibroblast cells, after stimulation with SAG to activate Hh, SMO localizes into cilia. In contrast, in patients with *RPGRIP1L* mutations, ciliary SMO levels drop significantly, suggesting impairment
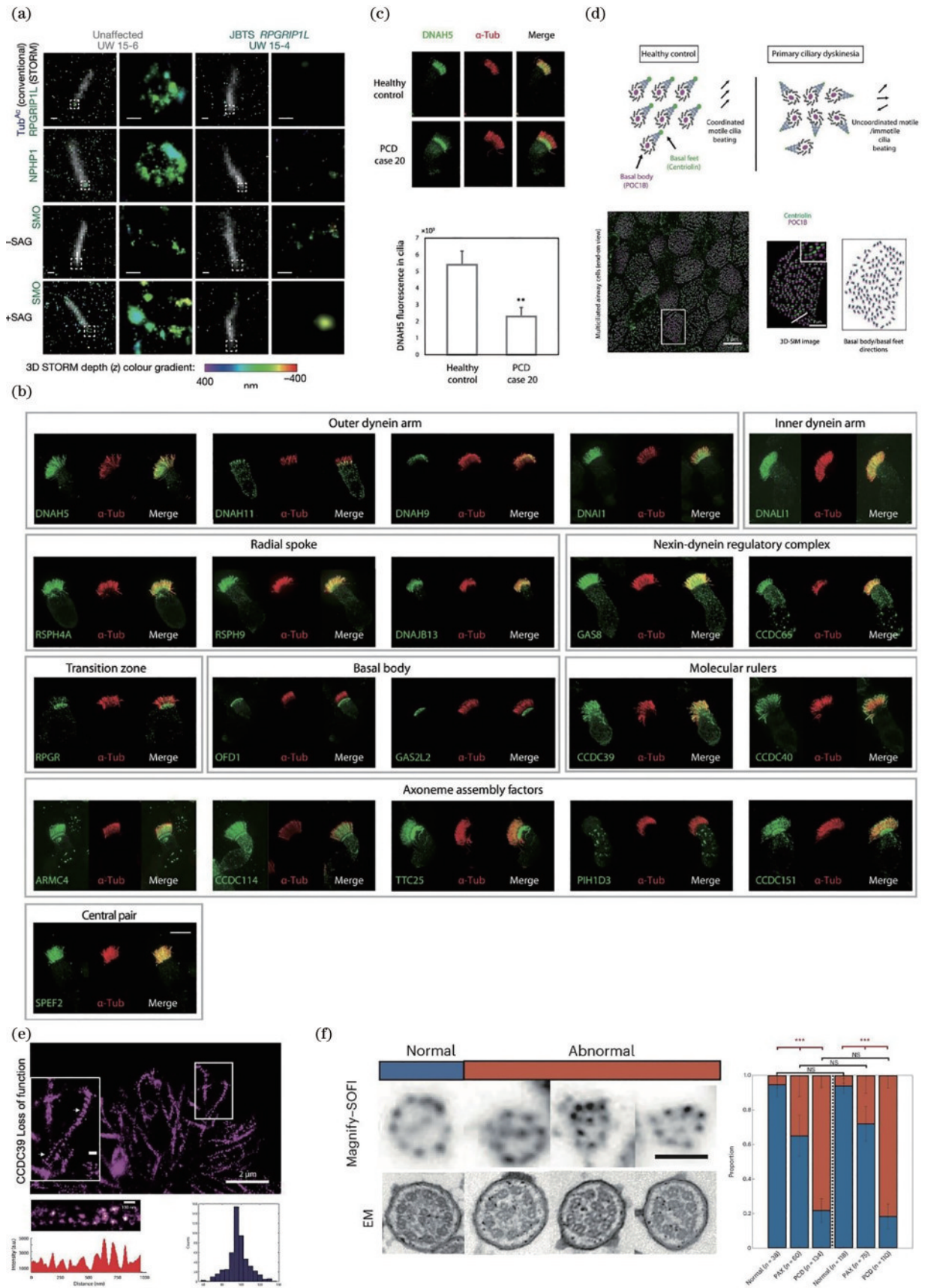
Fig. 4　Super-resolution imaging aids ciliopathy investigation and diagnostics. (a) 3D SIM reveals the disruption of the transition zone and impairment of Hh signaling in patients with JS[44]; (b) 3D SIM-based PCD molecular fingerprint for PCD diagnosis[40]; (c) PCD diagnosis based on quantitative 3D SIM[40]; (d) PCD diagnosis based on rotational polarity[40]; (e) STORM reveals the preservation of 96-nm periodicity in CCDC39 loss of function cells[40]; (f) PCD diagnosis based on MAGNIFY-SOFI[65]

of Hh signaling, as shown in Fig. 4(a). They also found diminished ciliary Arl13, another essential developmental regulator, in fibroblast cells from patients with either *RPGRIP1L* or *TCTN2* mutations. This study provides molecular insights into the pathology of JS, which involves disruption of the ciliary transition zone and Hh signaling, enabling cellular/molecular diagnosis.

5.2 PCD investigation and diagnosis using 3D SIM and STORM

Though rare, direct application of super-resolution imaging in disease diagnosis is possible, and PCD is one of the few examples that demonstrate the potential of super-resolution imaging. In the remaining sections, we focus on motile ciliopathy PCD. We first introduce the traditional methods of PCD diagnosis and then illustrate how super-resolution imaging improves the diagnosis. Finally, we discuss how the diagnosis can be further optimized by integrating multiplexed labeling and high-speed video microscopy (HSVM).

5.3 Different diagnostic approaches for PCD

Early diagnosis is essential for initiating therapies to slow PCD progression because a delay in diagnosis may lead to lung collapse or transplantation, threatening patients' lives. However, for a long time, PCD has been underdiagnosed because of its genetic heterogeneity, technical limitations, and lack of awareness. It may take years for patients with PCD to receive a confirmed diagnosis. Currently, two different methods are used to conclude the diagnosis: TEM and/or DNA sequencing. Even when the two techniques are combined, $\sim 30\%$ of patients with PCD clinical symptoms do not receive a confirmed diagnosis[59-60]. Unfortunately, a standalone approach for PCD diagnosis does not exist.

TEM was once regarded as the gold standard for PCD confirmation, specifically for ciliary ultrastructure defects. However, TEM mainly examines the absence of ODAs and/or IDAs, microtubule disorganization, and central pair defects and may introduce false-negative results. Generally, next-generation sequencing platforms enable the simultaneous querying of multiple exons, and compared with other methods, molecular genetic testing is an easy and quick option. However, unexpected mutations may occur in new PCD genes and untranslated regions, which can only be detected using the more expensive and time-consuming whole genome sequencing. Additionally, for known PCD causative genes, the mutations could be variants of unknown

significance (VUS), which are common and increase the complexity of the diagnosis.

Two other techniques have recently emerged to aid PCD diagnosis: HSVM and fluorescence microscopy. Ciliary beat information can be extracted from the HSVM of multiciliated cells; however, it is insufficient to confirm PCD. Most PCD diagnostics only examine the cilia beat frequency but do not adequately differentiate PCD because the cilia beat amplitude, waveform, and coordination are vital to evaluating the ciliary beat. Additionally, chronic infections can disable ciliary motility, leading to false-positive diagnosis.

5.4 PCD diagnosis using fluorescence microscopy and 3D SIM

For most motile ciliopathies, molecular defects impair the assembly of the sophisticated axoneme of cilia. Immunofluorescence can help illustrate the absence of these components and contribute to the diagnosis. Shoemark *et al*.[61] reported that fluorescence microscopy cannot be applied as a single standard for PCD diagnosis after examining 35 patients using 6 antibodies. However, their study was limited by the number of PCD antibodies, microscope resolution, and absence of image quantification.

To further validate the fluorescence microscopy-based diagnosis and increase the resolution, Liu *et al*. first generated a molecular fingerprint of ~ 25 PCD proteins by staining control multiciliated cells and using 3D SIM, as shown in Fig. 4(b). This super-resolution fingerprint reveals the subciliary distribution of PCD proteins in unprecedented detail, and examining PCD fingerprints from patients suspected of PCD can aid PCD diagnosis. They further developed an algorithm to quantitatively measure the abundance of certain proteins within motile cilia/multiciliated cells [Fig. 4(c)] and subsequently checked the multiciliated cells of 31 patients with PCD by super-resolution microscopy, including 39% of patients with unclear TEM diagnosis and 48% of patients with VUS. This result is promising because quantitative 3D SIM can diagnose these PCD cases. To automate the diagnostic pipeline, a machine learning-based classifier was further trained to distinguish PCD datasets from controls.

To test whether 3D SIM and antibody panel staining combination can be developed as an independent diagnostic tool, the authors further tested two patients with different antibody panels. The first patient with *DNAH5* and *DNAH11* mutations was diagnosed with 15 PCD protein antibodies, and the

result suggested the loss of all ODA components: DNAH5, DNAH11, and DNAI1. The second patient, with mutations in *DNAH11* and TEM inconclusive, was diagnosed with 10 PCD protein antibody panels, and the result suggested the absence of DNAH11.

When cilia beat coordinately, the basal feet point toward the direction of the cilia beat, a phenomenon called rotational polarity[62]. For patients with PCD, cilia lose beat or beat coordination; consequently, rotational polarity is disrupted. Rotational polarity can be measured by staining the basal body and foot markers. However, because of the close distance between the basal body and foot, conventional microscopy fails to distinguish the basal foot from the basal body. Liu *et al*.[40] showed clear basal foot signal separation from the basal body using 3D SIM [Fig. 4(d)]. They quantitatively measured rotational polarity in healthy controls and patients with PCD. The results show that rotational polarity is impaired in patients with PCD with *DNAH5*, *DNAH11*, or *HYDIN* mutations, whereas healthy controls and a patient with cystic fibrosis, another rare airway disease, maintain the polarity, suggesting a new approach to PCD diagnosis.

Antibody panel and quantitative 3D SIM-based diagnosis is straightforward and is likely to be implemented in clinical settings. Restricted by the availability of patients' cells, this study only examined 31 patients with the most common PCD mutations. The sensitivity and robustness of this method require more testing of more patients and PCD mutations in the future. Note that the more antibodies in the panel, the more patient cells and labor required. To address this issue, an antibody multiplexed labeling strategy is required to optimize diagnostics in the future.

5. 5 PCD investigation using 3D SIM and STORM

To further investigate whether super-resolution imaging can detect structural defects in patients with PCD, this study[40] focuses on patients with *CCDC39* mutations. CCDC39[63] is the human homolog of *Chlamydomonas* fap59, a molecular ruler of motile cilia that determines the transport of IDA and NDRC into cilia and the arrangement of the 96-nm periodicity of RS components[64]. Whether CCDC39 has the same function in human multiciliated cells was a point raised. The authors assessed the motile cilia from three patients with CCDC39 loss of function using 3D SIM and found that the IDA component DNALI1 and NDRC component GAS8 are trapped at the transition fiber rather than the transition zone. They further employed STORM to check the periodicity of RSPH4A and found that, unlike *Chlamydomonas*, it is unaffected after loss of CCDC39 in these three patients, whereas motile cilia present disorganized microtubules, as shown in Fig. 4(e). This result suggests the existence of different mechanisms or gene redundancy in humans.

5. 6 PCD diagnosis using MAGNIFY-SOFI

3D SIM-based diagnosis relies on sophisticated microscopes, which may not be accessible in many hospitals/institutes. Contrarily, expansion microscopy and SOFI can be performed using a regular fluorescence/confocal microscope.

To explore the possibility of applying expansion microscopy and SOFI to PCD diagnosis, Klimas *et al*.[65] developed an optimized expansion technique named MAGNIFY that expands the specimens up to 11-fold. When combined with second-order SOFI, MAGNIFY can achieve a resolution down to ~15 nm. They first used this technique to check motile cilia, and using a pan staining strategy that labels all proteins within a cell, the axoneme 9+2 structure was observed, and found to be similar to TEM micrographs shown in Fig. 4(f). They then examined human airway motile cilia treated with Taxol, a ligand that interferes with microtubule dynamics when administered in excessive doses. They identified disorganized microtubule doublets using MAGNIFY-SOFI, which previously could only be observed using TEM. They then examined the motile cilia from patients with *CCDC39* mutations and found a significant increase in the proportion of abnormal cilia [Fig. 4(f)].

This study provides an economical and speedy method for assessing the motile cilia architecture using super-resolution microscopy instead of TEM. TEM requires cutting samples into thin cross-sections and examining different cross-sections to locate motile cilia. MAGNIFY-SOFI is fluorescence imaging-based and does not involve sample cutting. However, this study was limited to pan staining of the entire motile cilia proteome. As molecular specificity is one major advantage of fluorescence microscopy, it would be encouraging to observe different components of the cilia axoneme stained by different antibodies and to compare the differences between healthy controls and patients with PCD in the future.

6 Future perspectives on ciliopathy diagnosis

Despite the exciting progress made by the two

groups, disease diagnosis using super-resolution microscopy is still at a preliminary stage.

One major challenge is the heterogeneity of the disease and the scarcity of patients. With the application of CRISPR KO in human airway cells, it would be helpful to test new and compare different diagnostics using CRISPR KO multiciliated cells[66]. The second challenge is the sensitivity of the antibody panel. New antibodies can be added to the panel but with increased requirements for patient samples and labor. Alternatively, multiplexed labeling approaches, such as DNA-PAINT[8], which can probe tens of targets easily and with single-cell sensitivity, can be adopted. The third challenge is data interpretation because antibody panel imaging produces large amounts of data. We anticipate that neural network-based image analysis can be applied to predict the results in the future.

Although the structure of cilia is well studied, their motility is only well characterized in a few model organisms and sperm cells. HSVM records ciliary motility with a high temporal resolution, and additional cilia beat parameters can be extracted to aid diagnosis. HSVM is also restricted by light microscopy resolution and sensitive cilia beat analysis which requires isolating a single cilium. Therefore, it is worthwhile to label motile cilia with fluorescent markers and apply high-speed super-resolution imaging techniques to distinguish single cilia for high-quality data analysis. Integrating cilia beat and antibody panel data will provide a more comprehensive characterization of cilia.

7 Summary

Super-resolution imaging has demonstrated its effectiveness in revealing the ciliary structure and diagnosing motile ciliopathy. The new generation of super-resolution imaging techniques that achieve nano- or angstrom spatial resolution and unprecedented time resolution are expected to revolutionize this field. High-speed super-resolution tracking techniques, such as MINFLUX[19] or MINSTED[67], can be applied to study cilia trafficking and cilia motor dynamics with single-molecule sensitivity. Combination of super-resolution imaging with other techniques, such as CryoET/CryoEM and CRISPR perturbation[68], to study the structural and functional changes in cilia in ciliopathies is also anticipated.

Regarding ciliopathy diagnosis, the sensitivity and accuracy of super-resolution imaging will be further evaluated by integrating patient data and checking CRISPR loss of function cells. The protocols can be further developed and optimized to facilitate diagnosis. Given that motile cilia are such sophisticated structures that they may reflect any cilia defects and multiciliated cells are easily accessible, other ciliopathies, such as sensory ciliopathies, can be possibly diagnosed by examining airway multiciliated cells.

Acknowledgement

Reference

[1] Huang B, Babcock H, Zhuang X W. Breaking the diffraction barrier: super-resolution imaging of cells[J]. Cell, 2010, 143(7): 1047-1058.

[2] Doksani Y, Wu J Y, de Lange T, et al. Super-resolution fluorescence imaging of telomeres reveals TRF2-dependent T-loop formation[J]. Cell, 2013, 155(2): 345-356.

[3] Jones S A, Shim S H, He J, et al. Fast, three-dimensional super-resolution imaging of live cells[J]. Nature Methods, 2011, 8: 499-508.

[4] Rust M J, Bates M, Zhuang X W. Sub-diffraction-limit imaging by stochastic optical reconstruction microscopy (STORM)[J]. Nature Methods, 2006, 3: 793-796.

[5] Betzig E, Patterson G H, Sougrat R, et al. Imaging intracellular fluorescent proteins at nanometer resolution [J]. Science, 2006, 313(5793): 1642-1645.

[6] Hess S T, Girirajan T P K, Mason M D. Ultra-high resolution imaging by fluorescence photoactivation localization microscopy[J]. Biophysical Journal, 2006, 91 (11): 4258-4272.

[7] Sharonov A, Hochstrasser R M. Wide-field subdiffraction imaging by accumulated binding of diffusing probes[J]. Proceedings of the National Academy of Sciences of the United States of America, 2006, 103 (50): 18911-18916.

[8] Jungmann R, Avendaño M S, Woehrstein J B, et al. Multiplexed 3D cellular super-resolution imaging with DNA-PAINT and Exchange-PAINT[J]. Nature Methods, 2014, 11: 313-318.

[9] Kner P, Chhun B B, Griffis E R, et al. Super-resolution video microscopy of live cells by structured illumination [J]. Nature Methods, 2009, 6: 339-342.

[10] Shao L, Kner P, Rego E H, et al. Super-resolution 3D microscopy of live whole cells using structured illumination[J]. Nature Methods, 2011, 8: 1044-1046.

[11] Gustafsson M G L, Shao L, Carlton P M, et al. Three-dimensional resolution doubling in wide-field fluorescence microscopy by structured illumination[J]. Biophysical Journal, 2008, 94(12): 4957-4970.

[12] Masch J M, Steffens H, Fischer J, et al. Robust

nanoscopy of a synaptic protein in living mice by organic-fluorophore labeling[J]. Proceedings of the National Academy of Sciences of the United States of America, 2018, 115(34): E8047-E8056.

[13] Böhm U, Hell S W, Schmidt R. 4Pi-RESOLFT nanoscopy[J]. Nature Communications, 2016, 7: 10504.

[14] Hofmann M, Eggeling C, Jakobs S, et al. Breaking the diffraction barrier in fluorescence microscopy at low light intensities by using reversibly photoswitchable proteins [J]. Proceedings of the National Academy of Sciences of the United States of America, 2005, 102(49): 17565-17569.

[15] Dertinger T, Colyer R, Iyer G, et al. Fast, background-free, 3D super-resolution optical fluctuation imaging (SOFI) [J]. Proceedings of the National Academy of Sciences of the United States of America, 2009, 106 (52): 22287-22292.

[16] Chen F, Tillberg P W, Boyden E S. Expansion microscopy[J]. Science, 2015, 347(6221): 543-548.

[17] Wassie A T, Zhao Y X, Boyden E S. Expansion microscopy: principles and uses in biological research[J]. Nature Methods, 2019, 16: 33-41.

[18] Chang J B, Chen F, Yoon Y G, et al. Iterative expansion microscopy[J]. Nature Methods, 2017, 14: 593-599.

[19] Balzarotti F, Eilers Y, Gwosch K C, et al. Nanometer resolution imaging and tracking of fluorescent molecules with minimal photon fluxes[J]. Science, 2017, 355 (6325): 606-612.

[20] Anvarian Z, Mykytyn K, Mukhopadhyay S, et al. Cellular signalling by primary cilia in development, organ function and disease[J]. Nature Reviews: Nephrology, 2019, 15(4): 199-219.

[21] Wang Y, Bernard A, Comblain F, et al. Melanocortin 4 receptor signals at the neuronal primary cilium to control food intake and body weight[J]. The Journal of Clinical Investigation, 2021, 131(9): e142064.

[22] Tu H Q, Li S, Xu Y L, et al. Rhythmic cilia changes support SCN neuron coherence in circadian clock[J]. Science, 2023, 380(6648): 972-979.

[23] Sheu S H, Upadhyayula S, Dupuy V, et al. A serotonergic axon-cilium synapse drives nuclear signaling to alter chromatin accessibility[J]. Cell, 2022, 185(18): 3390-3407.

[24] Bustamante-Marin X M, Ostrowski L E. Cilia and mucociliary clearance[J]. Cold Spring Harbor Perspectives in Biology, 2017, 9(4): a028241.

[25] Spassky N, Meunier A. The development and functions of multiciliated epithelia[J]. Nature Reviews: Molecular Cell Biology, 2017, 18(7): 423-436.

[26] Wallmeier J, Nielsen K G, Kuehni C E, et al. Motile ciliopathies[J]. Nature Reviews Disease Primers, 2020, 6: 77.

[27] Kuek L E, Lee R J. First contact: the role of respiratory cilia in host-pathogen interactions in the airways[J]. American Journal of Physiology: Lung Cellular and Molecular Physiology, 2020, 319(4): L603-L619.

[28] Hill D B, Swaminathan V, Estes A, et al. Force generation and dynamics of individual cilia under external loading[J]. Biophysical Journal, 2010, 98(1): 57-66.

[29] Ringers C, Olstad E W, Jurisch-Yaksi N. The role of motile cilia in the development and physiology of the nervous system[J]. Philosophical Transactions of the Royal Society B: Biological Sciences, 2020, 375(1792): 20190156.

[30] Fliegauf M, Benzing T, Omran H. When cilia go bad: cilia defects and ciliopathies[J]. Nature Reviews: Molecular Cell Biology, 2007, 8(11): 880-893.

[31] Kagan K O, Dufke A, Gembruch U. Renal cystic disease and associated ciliopathies[J]. Current Opinion in Obstetrics & Gynecology, 2017, 29(2): 85-94.

[32] Wu K Y, Tang F L, Lee D, et al. Ependymal Vps35 promotes ependymal cell differentiation and survival, suppresses microglial activation, and prevents neonatal hydrocephalus[J]. The Journal of Neuroscience, 2020, 40 (19): 3862-3879.

[33] Johanson C E, Duncan J A, Klinge P M, et al. Multiplicity of cerebrospinal fluid functions: new challenges in health and disease[J]. Cerebrospinal Fluid Research, 2008, 5: 10.

[34] Reiter J F, Leroux M R. Genes and molecular pathways underpinning ciliopathies[J]. Nature Reviews: Molecular Cell Biology, 2017, 18(9): 533-547.

[35] Pioch C O, Connell D W, Shoemark A. Primary ciliary dyskinesia and bronchiectasis: new data and future challenges[J]. Archivos De Bronconeumologia, 2023, 59 (3): 134-136.

[36] Corbit K C, Aanstad P, Singla V, et al. Vertebrate Smoothened functions at the primary cilium[J]. Nature, 2005, 437(7061): 1018-1021.

[37] Mick D U, Rodrigues R B, Leib R D, et al. Proteomics of primary cilia by proximity labeling[J]. Developmental Cell, 2015, 35(4): 497-512.

[38] Walton T, Gui M, Velkova S, et al. Axonemal structures reveal mechanoregulatory and disease mechanisms[J]. Nature, 2023, 618(7965): 625-633.

[39] Chen Z, Shiozaki M, Haas K M, et al. De novo protein identification in mammalian sperm using *in situ* cryoelectron tomography and AlphaFold2 docking[J]. Cell, 2023, 186(23): 5041-5053.

[40] Liu Z, Nguyen Q P H, Guan Q, et al. A quantitative super-resolution imaging toolbox for diagnosis of motile ciliopathies[J]. Science Translational Medicine, 2020, 12 (535): eaay0071.

[41] Gonçalves J, Pelletier L. The ciliary transition zone: finding the pieces and assembling the gate[J]. Molecules and Cells, 2017, 40(4): 243-253.

[42] Garcia-Gonzalo F R, Reiter J F. Open sesame: how transition fibers and the transition zone control ciliary composition[J]. Cold Spring Harbor Perspectives in Biology, 2017, 9(2): a028134.

[43] Tony Yang T, Su J, Wang W J, et al. Superresolution pattern recognition reveals the architectural map of the ciliary transition zone[J]. Scientific Reports, 2015, 5:

14096.

[44] Shi X Y, Garcia G III, van de Weghe J C, et al. Super-resolution microscopy reveals that disruption of ciliary transition-zone architecture causes Joubert syndrome[J]. Nature Cell Biology, 2017, 19(10): 1178-1188.

[45] Lambacher N J, Bruel A L, van Dam T J P, et al. TMEM107 recruits ciliopathy proteins to subdomains of the ciliary transition zone and causes Joubert syndrome [J]. Nature Cell Biology, 2016, 18(1): 122-131.

[46] Lancaster M A, Gopal D J, Kim J, et al. Defective Wnt-dependent cerebellar midline fusion in a mouse model of Joubert syndrome[J]. Nature Medicine, 2011, 17(6): 726-731.

[47] Moye A R, Robichaux M A, Wensel T. Expansion microscopy of mouse photoreceptor cilia[M]//Ash J D, Pierce E, Anderson R E, et al. Retinal degenerative diseases XIX. Advances in experimental medicine and biology. Cham: Springer, 2023, 1415: 395-402.

[48] Louvel V, Haase R, Mercey O, et al. iU-ExM: nanoscopy of organelles and tissues with iterative ultrastructure expansion microscopy[J]. Nature Communications, 2023, 14: 7893.

[49] Bowler M, Kong D, Sun S F, et al. High-resolution characterization of centriole distal appendage morphology and dynamics by correlative STORM and electron microscopy[J]. Nature Communications, 2019, 10: 993.

[50] Nguyen Q P H, Zhen L, Albulescu A, et al. Comparative super-resolution mapping of basal feet reveals a modular but distinct architecture in primary and motile cilia[J]. Developmental Cell, 2020, 55(2): 209-223.

[51] Liu Z, Nguyen Q P H, Nanjundappa R, et al. Super-resolution microscopy and FIB-SEM imaging reveal parental centriole-derived, hybrid cilium in mammalian multiciliated cells[J]. Developmental Cell, 2020, 55(2): 224-236.

[52] Mönnich M, Borgeskov L, Breslin L, et al. CEP128 localizes to the subdistal appendages of the mother centriole and regulates TGF-β/BMP signaling at the primary cilium[J]. Cell Reports, 2018, 22(10): 2584-2592.

[53] Mazo G, Soplop N, Wang W J, et al. Spatial control of primary ciliogenesis by subdistal appendages alters sensation-associated properties of cilia[J]. Developmental Cell, 2016, 39(4): 424-437.

[54] Yoon J, Comerci C J, Weiss L E, et al. Revealing nanoscale morphology of the primary cilium using super-resolution fluorescence microscopy[J]. Biophysical Journal, 2019, 116(2): 319-329.

[55] Chung J J, Shim S H, Everley R A, et al. Structurally distinct Ca^{2+} signaling domains of sperm flagella orchestrate tyrosine phosphorylation and motility[J].

[56] Cell, 2014, 157(4): 808-822.

Miller M R, Kenny S J, Mannowetz N, et al. Asymmetrically positioned flagellar control units regulate human sperm rotation[J]. Cell Reports, 2018, 24(10): 2606-2613.

[57] Liu P W, Lou X C, Wingfield J L, et al. Chlamydomonas PKD2 organizes mastigonemes, hair-like glycoprotein polymers on cilia[J]. Journal of Cell Biology, 2020, 219(6): 202001122.

[58] Liu C, Wang Q C, Gu L S, et al. CCDC176 stabilizes microtubule doublets 1 and 9 to ensure proper sperm movement[J]. Current Biology: CB, 2023, 33(16): 3371-3388.

[59] Shapiro A, Davis S, Polineni D, et al. Diagnosis of primary ciliary dyskinesia. an official American thoracic society clinical practice guideline[J]. American Journal of Respiratory and Critical Care Medicine, 2018, 197: e24-e39.

[60] Marshall C R, Scherer S W, Zariwala M A, et al. Whole-exome sequencing and targeted copy number analysis in primary ciliary dyskinesia[J]. G3, 2015, 5(8): 1775-1781.

[61] Shoemark A, Frost E, Dixon M, et al. Accuracy of immunofluorescence in the diagnosis of primary ciliary dyskinesia[J]. American Journal of Respiratory and Critical Care Medicine, 2017, 196(1): 94-101.

[62] Mitchell B, Jacobs R, Li J L, et al. A positive feedback mechanism governs the polarity and motion of motile cilia [J]. Nature, 2007, 447(7140): 97-101.

[63] Merveille A C, Davis E E, Becker-Heck A, et al. CCDC39 is required for assembly of inner dynein arms and the dynein regulatory complex and for normal ciliary motility in humans and dogs[J]. Nature Genetics, 2011, 43(1): 72-78.

[64] Oda T, Yanagisawa H, Kamiya R, et al. A molecular ruler determines the repeat length in eukaryotic cilia and flagella[J]. Science, 2014, 346(6211): 857-860.

[65] Klimas A, Gallagher B R, Wijesekara P, et al. Magnify is a universal molecular anchoring strategy for expansion microscopy[J]. Nature Biotechnology, 2023, 41(6): 858-869.

[66] Everman J L, Rios C, Seibold M A. Primary airway epithelial cell gene editing using CRISPR-Cas9[J]. Methods in Molecular Biology, 2018, 1706: 267-292.

[67] Weber M, von der Emde H, Leutenegger M, et al. MINSTED nanoscopy enters the Ångström localization range[J]. Nature Biotechnology, 2023, 41: 569-576.

[68] Breslow D K, Hoogendoorn S, Kopp A R, et al. A CRISPR-based screen for Hedgehog signaling provides insights into ciliary function and ciliopathies[J]. Nature Genetics, 2018, 50(3): 460-471.